



Review

Polylactic Acid Polymer Matrix (Pla) Biocomposites with Plant Fibers for Manufacturing 3D Printing Filaments: A Review

Victor Hugo M. Almeida ^{1,*} , Raldo M. Jesus ^{1,2,3} , Gregório M. Santana ² and Thaís B. Pereira ¹

¹ Postgraduate Program in Development and Environment, Santa Cruz State University—UESC, Jorge Amado Highway, Km 16, Ilhéus 45662-900, BA, Brazil; rmota@uesc.br (R.M.J.); thais_tbp@hotmail.com (T.B.P.)

² Department of Exact and Technological Sciences, Santa Cruz State University—UESC, Jorge Amado Highway, Km 16, Ilhéus 45662-900, BA, Brazil; gregorioengflorestal@gmail.com

³ National Institute of Science and Technology in Energy and Environment—INCT, Federal University of Bahia, Salvador 40170-115, BA, Brazil

* Correspondence: vhm Almeida@uesc.br

Abstract: The escalating global demand for polymer products and the consequent disposal challenge necessitate technological and sustainable solutions. Recent advances in the development of materials used in 3D printing equipment are described in this review, with a focus on new biocomposite materials. The investigation delves into biocomposites comprising PLA and its blends with other polymers, reinforced by plant fibers, with a particular focus on research conducted over the last five years. The information related to the raw materials' physical, chemical, and processing properties necessary for creating biocomposite filament and printed parts were summarized. The best results in terms of tensile and flexural strength were presented and discussed, signposting future research avenues and desirable objectives. The findings elucidate that the inclusion of plant fibers led to a reduction in mechanical strength relative to pure PLA; however, when smaller particle sizes of plant fibers were added in volumes below 10%, it resulted in improved performance. Moreover, physical and/or chemical pretreatment of fibers, along with the isolation of cellulose fibrils, emerged as pivotal strategies for bolstering mechanical strengths. Noteworthy are the promising prospects presented by the incorporation of additives, while the refinement of printing parameters is key to improving the tensile and flexural strength of printed components.

Keywords: additive manufacturing; bioplastics; lignocellulosic materials; natural fiber; composites



Citation: Almeida, V.H.M.; Jesus, R.M.; Santana, G.M.; Pereira, T.B. Polylactic Acid Polymer Matrix (Pla) Biocomposites with Plant Fibers for Manufacturing 3D Printing Filaments: A Review. *J. Compos. Sci.* **2024**, *8*, 67. <https://doi.org/10.3390/jcs8020067>

Academic Editor: Francesco Tornabene

Received: 11 October 2023

Revised: 24 October 2023

Accepted: 1 November 2023

Published: 9 February 2024



Copyright: © 2024 by the authors. Licensee MDPI, Basel, Switzerland. This article is an open access article distributed under the terms and conditions of the Creative Commons Attribution (CC BY) license (<https://creativecommons.org/licenses/by/4.0/>).

1. Introduction

Global polymer production in 2020 was over 367 million metric tons, and estimates show that this consumption will double by 2050 [1]. Bioplastics, such as PLA, are biodegradable, renewable, and sustainable alternatives to petroleum-derived plastics, that can also be applied in fiber-reinforced polymeric composites. PLA global production was around 190,000 tons in 2019 [2].

Fiber-reinforced polymer composites have been used for a wide variety of applications, requiring excellent mechanical properties, being initially developed for the aerospace industry (high-performance or advanced composites), but also found in automotive parts [3], electronic components [4,5], building materials [6], and specialized sports products' applications [7]. However, there are applications, such as household appliances [8], consumer products with metallic coating [9], packaging [10], automotive parts [11], and sports equipment [12], that do not require the excellent mechanical properties of advanced composites, making room for the use of natural fibers, especially plant-based ones [13,14].

Plant fibers, including wood dust [15–17], linen [18], lignocellulose [19], microfibrils [20], and cellulose nanofibrils [21,22], are being explored as functional additives and reinforcements in thermoplastics and thermosets used in 3D printing [23,24].

Over the last decades, 3D printing processes have been the subject of research in both academia and industry, with a focus on processing techniques and development of pure polymeric materials [25,26]. More recently, we are seeing considerable advances in the development of printable polymeric biocomposites with improved performance [27,28]. However, with the aim of mitigating environmental impacts, reducing costs, or improving chemical and physical properties in comparison with pure polymers, being able to produce parts with improved mechanics, reduced dimensional instability, and improved aesthetics, extensive research is being conducted to find the right materials, treatments, additives, and processes.

Recent advances in the development of materials used in 3D printing equipment are described in this review, focusing on new biocomposite materials.

2. Materials and Methods

Studies on biocomposites of PLA and its blends with other polymers, reinforced with plant fibers, were analyzed, and the works of the last five years were considered in this review, conducting consultations of articles/reviews in the databases Scopus, Scielo, Science Direct, and Wiley Journals. The Boolean operator “AND” was used to include multiple keywords in a single search. The keywords “3D printing”, “Additive manufacturing”, “Natural fibers”, and “PLA” were used.

The analysis of publications considered the key terms, whether they were present in the title, abstract, or keywords. In some cases, the whole text was inspected. After this initial research of biocomposites found in the scientific literature, 36 studies were selected that used the thermoplastic biopolymer PLA and its blends with other polymers, filled with plant fibers or lignocellulosic materials of plant origin, used as filaments in 3D printing equipment.

The information related to the physical, chemical, and processing properties of the raw materials to create the biocomposite, filament, and printed parts were summarized, and the best results regarding tensile and bending strength were presented and discussed.

3. Results

In this section, information will be presented about the processing of the fibers, the biocomposites, the printing parameters of the specimens, the tests carried out, and their results.

3.1. Biocomposites

The biocomposites studied in this review are polymer matrix PLA or PLA blends with other polymers, combined with plant fibers, and in some cases, they include additives.

The morphology and powder preparation of the plant fibers are critical elements for obtaining high-performance composites in the form of filaments for 3D printers. The size of the particles can pose a technological obstacle regarding the diameter of the extruder nozzle; in fact, all the studies analyzed in this review report having to crush and sieve the fibers at least once. In some studies, other physical and/or chemical pretreatments were applied to the fibers to improve interfacial bonding with the polymer matrix. Another way of improving polymer/fiber bonding are additive materials, which can be called plasticizers, coupling agents, lubricants, or graft polymers.

Table 1 summarizes information on the fibers used, including their average diameter after crushing and sieving, any pretreatment methods when applied, the polymer matrix, and the additives.

Table 1. Information on the component materials of the studied biocomposites.

Fiber (Acronym)	Average Fiber Diameter (μm)	Fiber Pretreatment	Polymeric Matrix	Additives in the Biocomposite	Source
Harakeke fiber (HKF)	12	5% NaOH and 2% Sodium Sulphite	PLA Ingeo™ 3052D	-	[29]
Hemp fiber (HF)	28	5% NaOH			
Poplar wood flour (PWF)	95 to 105	-	PLA	Glycerol Tributyl citrate	[30]
Cork powder (CP)	272 to 733	-	PLA Ingeo™ 4032D	Tributyl citrate	[15]
Wood powder (WP)	-	-	PLA	-	[17]
Poplar wood flour (WF)	149	-	PLA Ingeo™ 4032D	Polyurethane PCL POE Glycidyl methacrylate DCP	[31]
Beech wood (BW)	237	-	PLA Ingeo™ 2003D	-	[16]
Pinewood fiber (PW)	-	-	PLA	Polyhydroxyalkanoate -	[32]
Wood Fiber (WF)	-	-	PLA	-	[33]
Cedar wood fiber (WF)	-	-	PLA	-	[34]
Wood fiber (WF)	-	-	PLA	-	[34]
Flax fiber (FF)	20 to 650		PLA Ingeo™ 7001D	Polybutylene succinate	[18]
Flax shives (FS)	162 to 220				
Pinewood fiber (PW)	-	-	PLA	PHA-	[35]
Camargue rice husks (RHF)	28	-	PLA Ingeo™ 3001D	-	[36]
Pinus wood flour (WF)	209				
Raw sugarcane bagasse fiber (RSCB)	177	-			
Cellulose from sugarcane (SCBF)	177	7.5 wt.% NaOH 1% (w/v) NaClO ₂ Glacial acetic acid	PLA Ingeo™ 4032D	-	[20]
Cellulose nanofibrils (CNF) from sisal	0.01 to 0.05	5% (wt.% NaOH 1.5 wt.% NaClO, 7 g NaOH, and 75 mL glacial acetic acid	PLA Ingeo™ 3051D	Dimethylformamide and chloroform	[21]
Poplar wood (PW)	43	-	PLA Ingeo™ 4043D	-	[37]
Wood fiber (WF)	250	-	PLA Ingeo™ 4043D	-	[38]
Cellulose nanocrystals (CNC)	0.005 to 0.02	-	PLA Ingeo™ 2003D	-	[39]
Pennisetum		1.5% (w/v) of H ₂ SO ₄			
Silvergrass (SG)	20–40	3% (v/v) H ₂ O ₂ , 1.5% (w/v) NaOH, and 12.5 g/L Na ₂ SiO ₃	PLA Ingeo™ 4032D	-	[40]
Switch grass		Steam explosion			
Reed grass					
Cork	20–40	-	PLA Ingeo™ 4032D	MA	[41]

Table 1. Cont.

Fiber (Acronym)	Average Fiber Diameter (μm)	Fiber Pretreatment	Polymeric Matrix	Additives in the Biocomposite	Source
Cellulose nanofibrils (CNF)	0.05	Acetic acid-sodium acetate buffer and 0.5 mL cellic CTec2 High-pressure homogenization	PLA Ingeo™ 4032D	PEG600	[22]
Particleboard wood flour (PWF)	30	30 gr NaOH 30 wt.% H ₂ O ₂	PLA Ingeo™ 4032D	-	[42]
Wood powder (WP)	-	-	PLA	-	[43]
Agave fiber (AF)	36.6	-	PLA Ingeo™ 3051D	-	[44]
Lemongrass fiber (LF)	65.6	-	PLA Ingeo™ 4032D	MA	[45]
Oil Palm empty fruit bunch fibers (OPEFBF)	500	-	PLA Ingeo™ 2003D	-	[46]
Rice straw powder (RSP)	100	5 wt.% NaOH 1 wt.% acetic acid Ultrasound	PLA Ingeo™ 3052D	-	[47]
Olive wood bark (OW_b)	250	-	PLA Ingeo™ 4043D	-	[48]
Coconut fiber (CF)	297	Steam Explosion	PLA Ingeo™ 4043D	PBS	[49]
Walnut shell powder (WSP)	100	-	PLA	-	[50]
Walnut shell powder (WSP)	90	-	PLA	-	[51]
Eggshell powder (ESP)	-	-	-	-	-
Pineapple leaf fiber (PALF)	-	-	-	-	-
Pineapple leaf fiber (APALF)	-	6 wt.% NaOH Acetic acid	PLA Ingeo™ 4043D	-	[52]
Bamboo (B)	18.5 to 22.9	-	-	-	-
Pinewood (PW)	31.4 to 77.6	-	PLA	-	[53]
Cork (C)	11.2–12.7	-	-	-	-
Walnut shell (WS)	50	-	PLA Ingeo™ 3D850	Tri vinyl ethoxy silane	[54]
Hedysarum coronarium (HC) flour	150	-	PLA Ingeo™ 2003D	-	[55]
Kenaf (K)	250	-	PLA Ingeo™ 2003D	-	[56]
Rice husk (RH)	50	2 wt.% NaOH Silane KH550 and ethanol	PLA Ingeo™ 4032D	KH570	[57]

The polylactic acid (PLA) biopolymer was the polymer matrix considered in this study, as it is one of the most used polymers in Fused Filament Fabrication (FFF) 3D printing processes.

Various plant fibers were employed, such as wood fibers [16,17,30,32,34,35], cork dust [15,53], rice straw fibers [47], sugarcane bagasse [20], bamboo [53], grasses [40], sisal [21], linen [18], and hemp and harakeke [29].

The size of the particles used is an important variable to obtain a biocomposite with satisfactory performance. Yu's study [47] initially investigated the particle size used in the biocomposites. Rice straw fibers were crushed and sieved into four different particle sizes and applied in the formulation of the biocomposites. The results obtained in the mechanical tests demonstrated that this is an important variable for a good interaction between the

polymer and the reinforcing fiber to occur. Particle sizes of 250 μm (60#), 125 μm (120#), 97 μm (160#), and 74 μm (200#) were tested. The best mechanical properties were achieved with particles smaller than 125 μm (120#). According to the authors' analysis, the largest particle used (250 μm) had a roughened surface with defects in the fiber structure itself and did not disperse uniformly in the matrix, resulting in lower mechanical properties. Smaller-sized particles (125 μm) have a larger specific surface and had fewer internal defects and dispersed more evenly. In addition, interfacial bonding became stronger and better mechanical properties were obtained. However, the smaller particles (74 and 97 μm) may present unwanted agglomerations, making dispersion difficult, generating places of stress concentration and possible defects in the printed part.

In addition to particle size, separating cellulose microfibrils from other components of fibers, such as lignin, pectin, hemicellulose, minerals, and other elements, can enhance the stability of the composite. Some of these components may degrade at temperatures exceeding 150 $^{\circ}\text{C}$, leading to chemical reactions and the production of oxidation products, including alcohols, acids, or other volatile substances. Among the available surface modification methods, acid, alkali, and steam explosion treatments offer simple and cost-effective options for the removal of amorphous materials [40].

There are other methods, and each has its advantages and disadvantages, so it is desirable to use simple, non-polluting, and effective pretreatment processes. The toxicity of organic solvents, the higher energy consumption in microwave radiation, high-pressure homogenization, and the high price of wet and ionic liquid oxidation processes are examples of disadvantages for large-scale industrial applications of existing pretreatments.

Acid treatment and high-pressure homogenization were used in [22]. The acidic solution removed a good part of other components by isolating the cellulose fibrils. The high-pressure homogenization reduced the particle size, obtaining fibrils of a few hundred nanometers to 1 micron in length and an average diameter of less than 50 nm. However, in the formation of the biocomposite, agglomerations of cellulose fibrils occurred, resulting in blockages in the extrusion of the filament. Acid and/or alkaline treatments have also been used in [20,22,42,47] to remove lignin, hemicellulose, wax, and oils. Depending on the amount and concentrations, these baths can also depolymerize the cellulose structure by separating the cellulose microfibrils into shorter-length crystallites.

In Yu's study [47], combining two pretreatments—alkaline and ultrasonic—resulted in an improved mechanical performance of the printed samples. The authors attribute this improvement to the enhanced interfacial adhesion between the polymer and the fiber. Specifically, there was an approximately 18.75% increase in flexural strength, a 25.27% increase in flexural modulus, a 31.19% increase in tensile strength, and a 16.48% increase in Young's modulus when comparing the treated biocomposite to the untreated one.

Another way to improve the performance of these biocomposites is with the use of additives, which can reduce interfacial energy, improve dispersion by avoiding agglomeration of the fibers, improve interphase adhesion, and change the viscosity of the molten material, as well as the glass transition temperature (T_g), the melting temperature (T_m), and the elastic modulus, among others. These additives can be positioned between the sequences of the polymer chains, decreasing the interactions between them, thus increasing the free volume of the original polymer chains and influencing the attenuation of van der Waals bonds, resulting in a more flexible and extensible matrix. Depending on the molecular structure or the volume inserted, it can be allocated in the free space between the polymer chains, causing movement restriction and a consequent increase in stiffness and tensile strength, and a decrease in deformation at break and impact resistance.

In Xie's study [30], two plasticizers, glycerol (GRO) and tributyl citrate (TBC), were employed. Three combinations were analyzed: a PLA sample with 4% GRO (by weight), a second PLA sample with 2% GRO and 2% TBC (both by weight), and a third PLA sample with 4% TBC (by weight). The SEM images showed that in the composites with the GRO plasticizer and the mixture of GRO and TBC, it was possible to clearly identify the fiber particles, the polymer, and its borders, while with the TBC plasticizer (4 wt.%) there was an

improvement in the dispersion and interaction between the fiber and the polymer, as no clear and prominent fiber particles were visualized, nor were there clear limits between the fiber and the polymer. There was also an improvement in the adhesion between the fiber and the polymer, resulting in increased tensile strength and elongation at break compared to PLA/GRO and PLA/GRO + TBC, corroborating that there was improved interfacial adhesion.

The TBC plasticizer was also used by Daver [15], where the TBC plasticizer (5 wt.%) reduced tensile strength, compared to pure PLA and PLA with fiber. However, there was an increase in elongation at break, as in [30], probably due to the interaction of the fiber source used; in this case, cork, which despite being the bark of a tree, unlike fibers formed by cellulose, is formed mainly by suberin, which is a polymer of the polyester family and gives cork a viscoelastic behavior close to an elastomer.

In [31], thermoplastic polyurethane (TPU) was incorporated as an additive in the biocomposite of PLA and wood flour (WF). TPU is a multi-block copolymer of the (AB)_n type, featuring both soft segments (SS) and hard segments (HS). It can be thought of as an SS array with a dispersed phase comprising a separate HS domain. The SS sequences, which have a low glass transition temperature, are quite mobile and present an amorphous conformation at room temperature. HS sequences have a high melting temperature, are quite polar, and are fixed by intermolecular H-bonding. As a result, HS domains act as physical loads and crosslinks, while SS domains act as a matrix, that can yield high elasticity, transparency, and resistance to oils, grease, and abrasion. The TPU copolymer (10 wt.%) was able to improve the impact strength, tensile strength, and flexural strength by 51.31%, 33.98%, and 10.38%, respectively, relative to the PLA/WF biocomposite.

In the same study [31], a grafted copolymer (g) was employed as a compatibilizer. The synthesis took place through free radical polymerization with the presence of dicumyl peroxide (DCP) and the grafting of glycidyl methacrylate (GMA) into the PLA. This copolymer improved the interfacial bonding of the biocomposite, meaning that the epoxy groups present in the GMA chain can form strong hydrogen bonds with large numbers of hydroxyl groups of the fibers. Nitrogen in TPU carbamate can also form hydrogen bonds with hydroxyl groups on fibers. Through this coupling effect, the interface interaction between PLA, fiber (WF), and TPU was improved. The impact and tensile strength of the PLA/TPU/WFgGMA composite increased by 7.75% and 8.39%, respectively, in comparison to the PLA/WF/TPU composite. Polyethylene wax (PEWax—0.5 wt.%) was used as a lubricant to improve the process flowability during extrusion, preventing clogging and obstructions in the extrusion nozzle. Another graft copolymer (g), maleic anhydride (MA), was used as a compatibilizer in the biocomposite in [41] and in the work of [45].

In Ambone's study [21], cellulose nanofibers were mixed with dimethylformamide (DMF) as a solvent, and PLA was introduced into the solution with chloroform. The two solutions were subsequently combined and processed to create the PLA biocomposite with cellulose nanofibers (PLA/CNF). The tests with the printed PLA/CNF samples showed that there was an increase in the Young's modulus, tensile strength, and elongation at break, in comparison to the printed PLA samples. However, in addition to these solvents, the sisal fiber had been treated to obtain the cellulose nanofibers, so the resulting improvement in the final biocomposite had an influence on both the solvents used in the biocomposite mixing step and the chemical and mechanical pretreatments of the fibers.

In Wang's study [22], the additive helped to improve the dispersion of the fiber in the polymer matrix. The filament of the PLA biocomposite with nanocellulose was only successfully produced when polyethylene glycol 600 (PEG600 4 wt.%) was added. Following the addition of this plasticizer, the cellulose particles mixed more uniformly with the PLA, enabling the production of high-quality filaments. This would have been unattainable without this additive, as it prevented agglomerations of the cellulose particles and sporadic blockages during filament extrusion, thus averting bubble formation and ensuring a consistent filament diameter.

Table 2. Cont.

Diameter of Filament mm	Diameter of Nozzle mm	Layer Thickness mm	Infill %	Raster Angle (°)	Contour Layers	Speed Print mm.s ⁻¹	Printing Temp. °C	Bed Temp. °C	Source
1.75	0.4	0.25	-	±45	-	100	215	60	[51]
1.8	1.5	-	-	0/90	-	85	199	-	[52]
1.75	0.6	0.2	100	±45	-	45	200	50	[53]
1.75	0.4	0.3	100	-	2	30	230	60	[54]
1.75	0.4	0.1	100	±45	1	20	230	60	[55]
1.75	-	-	100	±45	-	60	200	50	[56]
1.75	0.6	0.2	-	±45	-	-	-	60	[57]

Each parameter has its degree of influence on the mechanical properties of the printed parts, with the layer thickness parameter being one of the most significant in the 3D printing process. In Ayrilmis’ study [34], four different layer thickness values (0.3 mm, 0.2 mm, 0.1 mm, and 0.05 mm) were compared. Thicker layers, as shown in Figure 1a, exhibit larger gaps between lines and layers, leading to increased porosity in the sample’s cross-section. This higher porosity resulted in greater water absorption. As the layer thickness decreased, there was an improvement in both tensile and flexural strength.

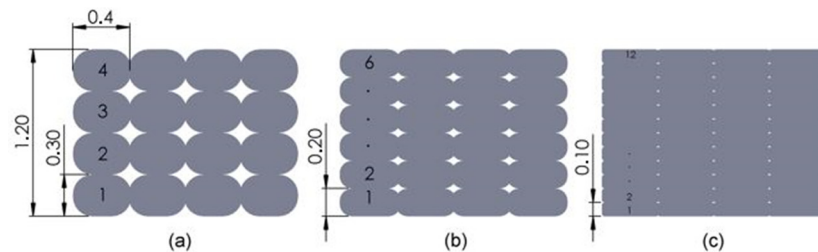


Figure 1. Illustration of printing with a 0.4 mm nozzle and different layer thicknesses: (a) 0.3 mm, (b) 0.2 mm, and (c) 0.1 mm.

As the layer thickness decreases while maintaining the final part thickness, the total number of layers increases. For example, in Figure 1, with a total height of 1.2 mm, you would need 4 layers with a thickness of 0.3 mm (Figure 1a), 6 layers with a thickness of 0.2 mm (Figure 1b), 12 layers with a thickness of 0.1 mm (Figure 1c), and so on. The experimental results demonstrated that as the layer thickness decreases, the flexural and tensile strength increase. This is due to the presence of more layers, each thinner, which leads to a higher reheating frequency of the previous layers, reducing porosity and improving diffusion between each printing layer. Additionally, decreasing layer thickness has the added effect of reducing surface roughness [26,34].

Martikka’s study [32] evaluated the infill, with samples printed at both 23% and 55% infill. The results indicated a significantly higher tensile strength with 55% infill. Most of the reviewed studies employed 100% infill, demonstrating that higher infill results in fewer empty spaces and greater piece resistance.

The raster angle of the infill can impact the mechanical properties because the molecular chains of the PLA polymer and biocomposites align with the printing direction. In Le Guen’s study [36], angles of 0° and 90° were employed (see Figure 2a,b) in relation to the part’s length. This resulted in a decrease in modulus and flexural strength for the specimens printed with a 90° angle. This anisotropy of the mechanical properties in relation to the longitudinal (0°) and transverse (90°) printing directions occurs due to the lower interaction between layers, and at a 90° angle, they are sideways in relation to the direction of the force applied in the mechanical tests, causing detachment between layers.

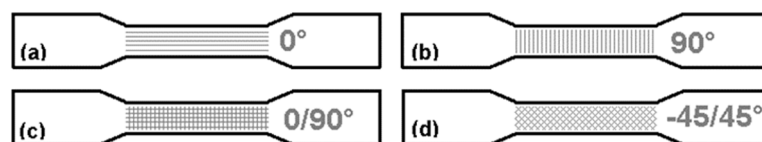


Figure 2. Illustration of the print angle (raster angle) of the internal filling (infill).

Liu [20] also examined the effect of the raster angle. In addition to the 0° and 90° angles, they analyzed the combination of alternating layers with $0/90^\circ$ and $-45/45^\circ$ angles (see Figure 2c,d). When considering tensile strength, samples printed at 0° demonstrated the best performance since the fibers and molecular chains aligned with the loading direction. Similar to Le Guen's findings [36], samples printed at 90° showed lower tensile strength. The $0/90^\circ$ and $-45/45^\circ$ configurations had results close to each other but slightly lower than the 0° samples. While the 0° configuration yielded better results, it may not always align with the demands and forces acting on the parts, making options with alternating layers at angles of $-45/45^\circ$ or $0/90^\circ$ appealing for part manufacturing.

The number of contour layers can directly influence the properties of mechanical strengths, as analyzed by Dong [17]. PLA and PLA/wood fiber samples were printed with two, four, and six contour layers, and the greater the number of layers, the greater the value of tensile strength and impact resistance.

The influence of printing speed was analyzed in [43]. The results were compared as a function of the variation of speeds at 30, 50, and $70 \text{ mm}\cdot\text{s}^{-1}$, while the other parameters remained unchanged. The results showed that the density of the printed part increased as the printing speed decreased, and the surface color became darker than that of the printed parts at high speed. The slow movement of the nozzle at a low printing speed resulted in more heating time of the wood fibers, leading to a darker part. The color variation of heat-treated wood is related to changes in compounds, such as the formation of oxidation products, and from hemicellulose decomposition. The printing speed did not significantly influence the tensile and flexural properties, while the modulus and compressive strength of the printed part significantly decreased by 14.6% and 34.3%, respectively, when the printing speed was increased from 30 to $70 \text{ mm}\cdot\text{s}^{-1}$. With a low printing speed, the material is exposed to heating for longer, resulting in adjacent overlapping layers with a better connection between them and, therefore, better compression performance.

Printing temperature plays a significant role in the properties of printed materials. In Guessasma's study [35], five different printing temperatures (210°C , 220°C , 230°C , 240°C , and 250°C) were evaluated. A slight improvement in traction performance was observed when the printing temperature was set to 230°C . Printing temperatures above 230°C were not suitable, as they led to a reduction in tensile properties, likely due to the thermal degradation of wood fiber particles.

In Yang's study [33], four different printing temperatures were evaluated: 200°C , 210°C , 220°C , and 230°C . Here, the PLA filament with wood fiber showed better performance at a temperature of 200°C , in which the samples showed higher values of tensile and flexural strength. With higher temperatures (above 200°C), the tensile and flexural strengths showed a reduction. Again, this loss of tensile and flexural strength can be attributed to the formation of acidic products of hemicellulose degradation. These acids cause depolymerization, shortening of the cellulose polymer, and cleavage of the bonds at the interpolymer level [33].

3.3. Mechanical Tests

3.3.1. Tensile Tests

Table 3 displays the sample names, weight percentages of component elements, tensile strength, Young's modulus, elongation at break, and the reference technical standard. The sample names follow the abbreviations of each biocomposite material, as listed in Table 1. It is worth noting that in most studies, the samples were 3D-printed using filaments produced from the biocomposite. However, in some studies, the mechanical analyses were conducted

solely on the filaments, indicated by the symbol (*). When values were extracted from graphs or cited as approximations by the authors, they were marked with the symbol (~). The data were organized based on the order of the best tensile strength results of the generated biocomposites. When available, the tensile strength values of the PLA samples were also included.

Table 3. Composition of specimens and results of tensile tests.

Sample	Composition by Weight %	Tensile Strength (MPa)	Young's Modulus (MPa)	Elongation at Break %	Standard	Source
PLA	100	52.35	900	9.35		
PLA/PBS/CF	77/20/3	71.81	1120	10.27	ASTM D638	[49]
PLA	100	56	1260	10		
PLA/HC	90/10	63	1843	9	-	[55]
PLA	100	51.39	3030	8.7		
PLA/CNC	99/1	61.07	4550	2.87	ASTM D638	[39]
PLA	100	47.99	492.64	-		
PLA/FPA #120 AU	99/1	58.59	568.68	-	ISO 527	[47]
PLA	100	64.2	-	-		
PLA/SCBF	94/6	57.1	-	-	ISO 527	[20]
PLA	100	* 55	* 3270	-		
PLA/BW	90/10	* 57	* 3630	-	-	[16]
PLA	100	* ~46	-	* ~3		
PLA/PEG/CNF	97.5/2.5	* ~57	-	* ~4.5	-	[22]
PLA	100	56.36	-	-		
PLA/K	97/3	54.78	-	-	ASTM D638	[56]
PLA	100	59.6	-	-		
PLA/LF/gMA	90/5/5	54.0	-	-	ISO 527	[45]
PLA	100	48.46	-	-		
PLA/WSP/ESP	92.5/5/2.5	53.26	-	-	ASTM D638	[51]
PLA	100	43.79	760	7.0		
PLA/PWF	95/5	52.54	3340	8.52	ISO 527-3	[42]
PLA/WSP	97.5/2.5	* 50.13	-	24.62	-	[50]
PLA	100	60	2870	2.5		
PLA/PW	80/20	50	3630	1.5	ASTM D638	[37]
PLA	100	~51	~1100	-		
PLA/AF	97/3	~46	~1060	-	ASTM D638-03	[44]
PLA	100	40.8	3474	-		
PLA/WF	97.5/2.5	44.4	3608	-	ASTM D638	[38]
PLA	100	29.5	879.4	4.34		
PLA/APALF	97/3	42.9	1337.7	5.97		
PLA/PALF	97/3	42.3	1311.0	6.89	ASTM D638	[52]
PLA	100	22.37	2062.75	1.49		
PLA/CNF	99/1	41.15	3365.66	2.09	-	[21]
PLA	100	21.27	1030	-		
PLA/RH6/KH	94/6	38.70	2040	-	ASTM D638	[57]
PLA	100	~38	-	-		
PLA/TPU/WF/gGMA	78/10/10/2	~38	-	-	ASTM D638	[31]
PLA	100	~35	~2500	-		
PLA/HKF	80/20	~37	~4300	-		
PLA/HF	90/10	~38	~3400	-	-	[29]
PLA/Wood	70/30	35.5	3642	-	ISO 527	[34]
PLA	100	~48				
PLA/C/MAGPLA	81/15/4	~35			ISO 527-2	[41]
PLA/FF	90/10	34.2	3968	1.2		
PLA/PBS/FS	45/45/10	34.1	2190	1.3	ISO 527-1	[18]

Table 3. Cont.

Sample	Composition by Weight %	Tensile Strength (MPa)	Young's Modulus (MPa)	Elongation at Break %	Standard	Source
PLA/PC 5% TBC	95/5	30.53	2498	1.89	ASTM D638	[15]
PLA	100	59.3	-	-	-	[53]
PLA/PW	85/15	30.4	-	-	-	[54]
PLA/WS	90/10	27.04	-	-	ASTM D638	[40]
PLA/SG	90/10	26.94	720.36	-	GB/T 24508	[30]
PLA/PWF 4% TBC	70/30	24.6	-	1.77	GB/T 1040	[46]
PLA	100	* 35.9	* 1970	-	-	[35]
PLA/OPEFBF	90/10	* 22.79	* 1920	-	-	[33]
PLA/PHA/PW	70/30	20.8	446	6.7	ISO 527-1	[43]
PLA/WF	60/40	20.0	1802	-	ASTM D638	[17]
PLA/WP	60/40	19.8	1731	-	ASTM D638	
PLA	100	37.38	-	-	-	
PLA/WP	60/40	13.49	-	-	ASTM D638	
PLA	100	26.8	1800	-	-	
PLA/WF	70/30	7.3	700	-	-	
PLA/LW	60/40	4.8	300	-	EN ISO 527-1	[32]

* Tests performed only on the filament. ~ Approximated values.

An initial analysis of the tensile strength values of pure PLA samples across various studies revealed significant variation. The reported values range from a minimum of 22.37 MPa in [21] to a maximum of 64.2 MPa in [20]. This variation is primarily attributed to differences in printing parameters, and some notable trends will be discussed below.

Looking at the top-three tensile strength results of pure PLA samples (64.2 MPa [20], 59.3 MPa [53], and 56 MPa [55]), some patterns emerged. These high results were achieved by using high printing temperatures (200 °C, 200 °C, and 230 °C, respectively) and small layer thicknesses (0.1 mm, 0.2 mm, and 0.1 mm, respectively). The first two studies employed a 0.6 mm nozzle diameter, while the third used a 0.4 mm nozzle. All three used 100% infill. The printing speed showed the most variation, with values of 40 mm.s⁻¹, 45 mm.s⁻¹, and 20 mm.s⁻¹, respectively. The raster angles used in each study were 0°, -45/45°, and -45/45°, respectively.

Most samples were designed and tested following ASTM 638 [59] and ISO 527 [60] standards. In addition, GB/T 1040-92 [61] and GB/T 24508 [62] were cited in [40]. However, some studies did not mention or adhere to any specific technical standards, which makes it challenging to compare their mechanical test values with those from other works. For example, the second-best tensile strength result for a sample printed with the generated biocomposite was obtained in [55]. However, the format of this sample differs from that specified in the standards, making direct comparisons with other studies difficult. Nevertheless, the biocomposite sample demonstrated a 12.5% improvement in tensile strength and a 46% increase in the Young's modulus compared to pure PLA. In this study, the fibers were only crushed and sieved, with particle sizes smaller than 150 µm, without any pretreatment or additives. This contrasts with the usual trend of reduced tensile strength.

The addition of natural fibers is expected to increase the stiffness (Young's modulus) of a composite, just as the tensile strength is expected to decrease with the addition of fibers and to decrease more as the amount of fiber increases in comparison to the polymer in the biocomposite. This trend was seen in [29], where the biocomposite with 30% hemp fiber showed 38% lower tensile strength compared to the biocomposite with 10% fiber. This behavior also occurred in [17], where the sample of pure PLA presented a tensile strength of 37.38 MPa and the biocomposite with 60% fiber presented 13.49 MPa; that is, a reduction of 74%. In Martikka's study [32], the pure PLA sample presented a tensile strength of 26.8 MPa, the biocomposite with 30% fiber presented 7.3 MPa, and the biocomposite with

40% fiber presented 4.8 MPa; that is, a reduction of 72% and 82%, respectively. As in Yang's study [43], the biocomposite with 40% fiber obtained a tensile strength of 19.8 MPa.

The PLA/PBS/CF biocomposite (77/20/3 wt.%) reported in [49] achieved the highest tensile strength performance, at 71.81 MPa, among the standardized samples. Similar to the best tensile strength result of the 64.2 MPa pure PLA specimens in [20], this achievement was attributed to a high printing temperature (230 °C) and low layer thickness (0.1 mm), with a 1 mm-diameter nozzle, 100% infill, and a $-45/45^\circ$ raster angle. The significance of applying pretreatment to the fibers is also evident. In this study, the steam explosion (SE) process was used with coconut fibers (CF). The high temperatures, pressure, and steam velocity of this process break the fiber chains, facilitating the removal of a portion of the hemicellulose and resulting in smaller cellulose fibrils, as observed in [40]. Additionally, PBS polymer was incorporated alongside PLA in forming the PLA/PBS/CF biocomposite (77/20/3 wt.%), leading to a remarkable approximately 37% improvement in tensile strength over pure PLA. Another noteworthy factor was the fiber quantity used (3 wt.%), demonstrating that the best strength results typically occur with a lower fiber content in biocomposites.

Examining the second-highest tensile strength value (61.07 MPa) among the standardized samples, which was achieved with a PLA biocomposite containing cellulose nanocrystals (PLA/CNC) in [39], underscored the significance of particle size selection and fiber pretreatment. This study utilized cellulose nanocrystals with particles ranging from 5 to 20 nm. Additionally, a crucial factor was the low fiber content (1 wt.%), demonstrating that better mechanical results are often achieved with lower fiber quantities.

Examining the third-highest tensile strength value (58.59 MPa) among the standardized samples, achieved with a PLA biocomposite and rice straw fiber in [47], emphasized the role of particle size. In this study, the initial step involved identifying the ideal particle size, with four options analyzed. Particles smaller than 125 μm demonstrated the best tensile strength and Young's modulus values, being only 2% and 0.7% smaller than the pure PLA sample. Once the optimal particle size was determined, alkaline and ultrasonic pretreatments were applied to the fiber, resulting in an improved biocomposite performance. The biocomposite exhibited a tensile strength and Young's modulus 22% and 15% higher than those of pure PLA. As in previous cases, a low fiber content (1 wt.%) was used, supporting the trend that lower fiber quantities lead to better mechanical results.

Examining the fourth-best tensile strength result (57.1 MPa) among the standardized samples, achieved with a PLA biocomposite and sugarcane bagasse fiber [20], highlighted the advantage of chemical pretreatments in removing hemicellulose, lignin, pectins, and other components. The biocomposite with cellulose fibrils isolated from sugarcane bagasse fibers (PLA/SCBF) outperformed the biocomposite with untreated sugarcane bagasse fibers (PLA/RSCB). The printed PLA/SCBF biocomposite (94/6 wt.%) presented a tensile strength of approximately 53 MPa, while the printed PLA/RSCB biocomposite (94/6 wt.%) presented approximately 49 MPa; that is, the natural fiber presented a tensile strength 8% lower than the biocomposite with the cellulose fibrils isolated with the chemical pretreatments.

3.3.2. Bending Tests

Table 4 provides the names of the samples, the weight percentages of component elements, flexural strength values, flexural modulus, and the technical standards used. The sample names correspond to those cited in their respective original studies and consist of abbreviations of each biocomposite material, as listed in Table 1. Most of the samples were designed and tested following ASTM D790 [63] and ISO 178 [64] standards, with only one study using the GB/T 24508 [62] standard, and another not specifying any standard.

Table 4. Composition of specimens and results of bending tests.

Sample	Composition by Weight (%)	Flexural Strength (MPa)	Flexural Modulus (MPa)	Standard	Source
PLA/Wood	70/30	128.3	4887	ISO 178	[34]
PLA	100	102.3	2560		
PLA/PBS/F	77/20/3	106.9	3280	ASTM D790	[49]
PLA	100	98.3	2220		
PLA/LF/gMA	93/5/2	97.4	3252	ISO 178	[45]
PLA	100	~103	~3050		
PLA/SCBF	97/3	~91	~3150	ISO 178	[20]
PLA	100	77.62	2586.80		
PLA/FPA #120 AU	99/1	90.32	3218.12	ISO 178	[47]
PLA	100	81.18	-		
PLA/WSP/ESP	92.5/5/2.5	88.25	-	ASTM D790	[51]
PLA	100	65.21	760		
PLA/PWF	95/5	80.66	3340	ISO 178	[42]
PLA	100	87	3280		
PLA/AF	97/3	79	3374	ASTM D790	[44]
PLA	100	33	500		
PLA/HC	80/20	68	980	ASTM D790	[55]
PLA	100	~70	-		
PLA/TPU/WF	80/10/10	~60	-	ASTM D790	[31]
PLA	100	~73	~2300		
PLA/WF	90/10	~58	~2600		
PLA/RHF	90/10	~52	~2100	-	[36]
PLA	100	32.2	1027.4		
PLA/APALF	97/3	51.9	1966.0		
PLA/PALF	97/3	48.5	1499.9	ASTM D790	[52]
PLA	100	99.2	3200		
PLA/OWB	90/10	40.9	2100	ISO 178	[48]
PLA/WS	90/10	38.68	-	-	[54]
PLA/WF	60/40	35.2	1928	ASTM D790	[33]
PLA/WP	60/40	34.0	1680	ASTM D790	[43]
PLA	100	80.09	-		
PLA/WP	40/60	33.00	-	ASTM D790	[17]
PLA	100	20.95	1062		
PLA/RH6/KH	94/6	32.27	1710	ASTM D790	[57]
PLA/SG	90/10	29.89	946.83	GB/T 24508	[40]

~ Approximated values.

As with the tensile properties, the addition of vegetable fibers is expected to decrease the flexural strength and increase the flexural modulus, confirming the low interconnection of materials and increased fragile behavior. In [17], the flexural strength of the PLA was 80.09 MPa, while with the PLA/WP biocomposite (40/60 wt.%), the flexural strength decreased to 33.00 MPa, almost 60% lower.

In [31], the addition of fiber made the flexural strength drop from approximately 70 MPa in pure PLA to approximately 47 MPa in the PLA/WF biocomposite (90/10%), a reduction of more than 30%. However, there was an optimization in flexural strength when the TPU polymer was added. The biocomposite PLA/TPU/WF (80/10/10 wt.%) achieved a flexural strength of approximately 60 MPa, nearly reaching the value obtained with pure PLA. In the same study, an additional additive, glycidyl methacrylate (GMA) graft polymer, was introduced. However, unlike the positive effect of GMA on tensile strength, the flexural strength results in PLA/TPU/WFgGMA biocomposites were lower than those obtained with the PLA/TPU/WF biocomposite without the GMA graft polymer.

In [40], three distinct fiber pretreatment methods were examined to eliminate amorphous materials: acid treatment (AT), alkaline treatment (AH), and steam explosion treatment (SE). Among these, the biocomposites of fibers subjected to alkaline treatment exhibited superior flexural strength and flexural modulus. The results indicated a significant

reduction in lignin content following alkaline treatment, leading to the conclusion that lignin content plays a pivotal role in influencing flexural strength and modulus.

The study in [34] proved that the printing parameters can also change the values of strength and flexural modulus. Here, the parameter analyzed was layer thickness, with a flexural strength of 128.3 MPa for a print layer thickness of 0.05 mm and 84.3 MPa for a layer of 0.3 mm. This result is consistent with the discussion about layer thickness in Section 3.2 about printing samples parameters.

In [20], an improvement in flexural strength was seen when the cellulose fibrils were isolated from the other plant fiber materials. The PLA biocomposite with PLA/SCBF cellulose fibrils (97/3 wt.%) extracted from the sugarcane bagasse fibers showed flexural strength of approximately 91 MPa, while the PLA biocomposite with PLA/RSCB sugarcane bagasse fibers (97/3) showed flexural strength of approximately 88 MPa. However, the flexural strength results were lower than that of pure PLA (~103 MPa). Probably, the particle size or the percentage (wt3%) of fiber added were decisive, since in [47], the result of the flexural strength of the biocomposite was better than the result for pure PLA.

In [47], in addition to applying pretreatment for the removal of lignin and hemicellulose, four different particle sizes were tested at first, and after choosing the particle size (<#120), the alkaline and ultrasound pretreatments were applied. Another factor that may have been crucial was the lower percentage of added fiber in [47] in comparison to that in [20], at 1 wt.% and 3 wt.%, respectively. In [47], the flexural strength of the biocomposite PLA/FPA (99/1 wt.%) was 90.32 MPa, while that of pure PLA was 77.62 MPa, an increase of just over 16%.

4. Discussion

The production of 3D printing filaments using plant fibers and PLA offers several benefits, including the valorization of natural resources, the recycling of agricultural and furniture waste, and the broadening of material options, while reducing costs for FFF 3D printing technology.

Typically, the addition of plant fibers to the PLA matrix led to a decline in the mechanical properties of 3D-printed biocomposites. However, it did improve the Young's modulus and flexural modulus by increasing the stiffness of the biocomposite. Some results showed that the fibers can act as an auxiliary crystallization agent of PLA; however, due to the low affinity of the fiber and PLA surfaces, weak bonds occur that result in a reduction in tensile and flexural strength.

The amount of fiber particles added to the biocomposite is crucial for better results. The percentage by weight (wt.%) in relation to the PLA polymer varied between 1% and 60% in the reviewed studies, and the best results for the mechanical strengths were those with low amounts of fibers, usually between 1% and 10%. The opposite was also observed. The worst resistance values were obtained with the highest percentage values of fibers added, between 30% and 60%. Although weight amounts of fiber are low due to the inherent low density of the fibers, in comparison, the percentage by volume is generally much higher than the percentage by weight, e.g., for one of the biocomposites, the percentage by weight of fiber was 15%, equivalent to 55% of the volume of the biocomposite.

Particle size is a critical factor, and the best results were achieved with crushed and sieved particles smaller than 300 μm . Smaller particles have a larger specific surface area, which can lead to particle aggregations and challenges in achieving uniform dispersion. Additives can effectively address this issue, enhancing dispersion, preventing particle agglomeration, and improving the interfacial bonding between fibers and polymers. Additionally, additives can help enhance the viscosity of the biocomposite.

Considering the 3D printing process, the ratio of nozzle diameter and print layer thickness is crucial. Particles larger than 100 μm can pose challenges when printing 0.1 mm (100 μm) layers, which was the most commonly used layer thickness.

Another crucial factor is the chemical composition of the fibers. The presence of hemicelluloses, lignin, pectin, minerals, and other components can hinder interfacial

bonding. To enhance the biocomposite performance, it is essential to isolate cellulose fibrils through chemical and physical pretreatments. These pretreatments, either individually or in combination, dissolve the fibers, separating cellulose from other components and improving compatibility between the polymer matrix and cellulose fibers. In fact, the best results of mechanical strengths were obtained with fibers subjected to treatment, such as steam explosion, or in alkaline or acidic solutions.

The manufacture of filaments for 3D printing with PLA biocomposites and plant fibers is promising, considering that several positive results have been reported. Simple techniques for treating the fibers have been reported, providing significant improvements in their interaction with the polymer, as proven with mechanical strength values equal to or sometimes higher than the PLA-printed samples.

Using these plant fibers reduces the amount of polymeric raw material required for 3D printing, leading to a decrease in polymer consumption. This also offers the advantage of potentially reducing filament costs, as many of these fibers are low-cost and readily available in nature. Some are even by-products or rejects from industries such as agriculture, furniture, cosmetics, and food production.

Author Contributions: Conceptualization, investigation, writing original draft preparation, V.H.M.A.; Visualization, supervision, project administration, R.M.J.; Methodology, writing review and editing, formal analysis, G.M.S.; investigation, data curation, T.B.P. All authors have read and agreed to the published version of the manuscript.

Funding: This research received no external funding.

Acknowledgments: This work was funded for publication with financial support from the Office of Research and Postgraduate Studies at the State University of Santa Cruz.

Conflicts of Interest: The authors declare no conflict of interest.

References

1. Future Markets. *The Global Market for Bioplastics and Biopolymers 2023–2033*; Future Markets, Inc.: Edimburgo, UK, 2022.
2. De Oliveira, P.Z.; de Souza Vandenbergh, L.P.; de Mello, A.F.M.; Soccol, C.R. A concise update on major poly-lactic acid bio-processing barriers. *Bioresour. Technol. Rep.* **2022**, *18*, 101094.
3. Maia, B.S.; Behraves, A.H.; Tjong, J.; Sain, M. Mechanical performance of modified Polypropylene/Polyamide matrix reinforced with treated recycled carbon fibers for lightweight applications. *J. Polym. Res.* **2022**, *29*, 136.
4. Lyu, Z.; Lim, G.J.; Koh, J.J.; Li, Y.; Ma, Y.; Ding, J.; Wang, J.; Hu, Z.; Wang, J.; Chen, W.; et al. Design and Manufacture of 3D-Printed Batteries. *Joule* **2020**, *5*, 89–114. [[CrossRef](#)]
5. Tan, H.W.; Choong, Y.Y.C.; Kuo, C.N.; Low, H.Y.; Chua, C.K. 3D printed electronics: Processes, materials and future trends. *Prog. Mater. Sci.* **2022**, *127*, 100945.
6. Song, J.; Cao, M.; Cai, L.; Zhou, Y.; Chen, J.; Liu, S.; Zhou, B.; Lu, Y.; Zhang, J.; Long, W.; et al. 3D printed polymeric formwork for lattice cementitious composites. *J. Build. Eng.* **2021**, *43*, 103074. [[CrossRef](#)]
7. Bunsell, A.; Joannès, S.; Thionnet, A. *Fundamentals of Fibre Reinforced Composite Materials*; CRC Press: Boca Raton, FL, USA, 2021.
8. Mitra, B.C. Environment Friendly Composite Materials: Biocomposites and Green Composites. *Def. Sci. J.* **2014**, *64*, 244–261. [[CrossRef](#)]
9. De Almeida, V.H.M.; Pisani, M.B.; Camargo, J.C.; Sousa, E.F.M.; Gomes, V.; Almeida, E.C. Metallic Surface Coating of Polymeric Parts Produced by Additive Manufacturing Process. *Mater. Sci. Forum* **2020**, *1012*, 453–458. [[CrossRef](#)]
10. Escursell, S.; Llorach-Massana, P.; Roncero, M.B. Sustainability in e-commerce packaging: A review. *J. Clean. Prod.* **2020**, *280*, 124314. [[CrossRef](#)]
11. Diegel, O. Additive Manufacturing: An Overview. In *Comprehensive Materials Processing*; Saleem, H., Ed.; Elsevier: Amsterdam, The Netherlands, 2014; Volume 10, pp. 3–18.
12. Dicker, M.P.; Duckworth, P.F.; Baker, A.B.; Francois, G.; Hazzard, M.K.; Weaver, P.M. Green composites: A review of material attributes and complementary applications. *Compos. Part A Appl. Sci. Manuf.* **2014**, *56*, 280–289. [[CrossRef](#)]
13. Shekar, H.S.; Ramachandra, M.J.M.T.P. Green Composites: A Review. *Mater. Today Proc.* **2018**, *5*, 2518–2526.
14. Rafiee, K.; Schmitt, H.; Pleissner, D.; Kaur, G.; Brar, S.K. Biodegradable green composites: It's never too late to mend. *Curr. Opin. Green Sustain. Chem.* **2021**, *30*, 100482.
15. Daver, F.; Lee, K.P.M.; Brandt, M.; Shanks, R. Cork-PLA composite filaments for fused deposition modelling. *Compos. Sci. Technol.* **2018**, *168*, 230–237.
16. Kariz, M.; Sernek, M.; Obućina, M.; Kuzman, M.K. Effect of wood content in FDM filament on properties of 3D printed parts. *Mater. Today Commun.* **2018**, *14*, 135–140. [[CrossRef](#)]

17. Dong, Y.; Milentis, J.; Pramanik, A. Additive manufacturing of mechanical testing samples based on virgin poly (lactic acid) (PLA) and PLA/wood fibre composites. *Adv. Manuf.* **2018**, *6*, 71–82. [[CrossRef](#)]
18. Badouard, C.; Traon, F.; Denoual, C.; Mayer-Laigle, C.; Paës, G.; Bourmaud, A. Exploring mechanical properties of fully compostable flax reinforced composite filaments for 3D printing applications. *Ind. Crop. Prod.* **2019**, *135*, 246–250. [[CrossRef](#)]
19. Zarna, C.; Opedal, M.T.; Echtermeyer, A.T.; Chinga-Carrasco, G. Reinforcement ability of lignocellulosic components in biocomposites and their 3D printed applications—A review. *Compos. Part C Open Access* **2021**, *6*, 100171. [[CrossRef](#)]
20. Liu, H.; He, H.; Peng, X.; Huang, B.; Li, J. Three-dimensional printing of poly(lactic acid) bio-based composites with sugarcane bagasse fiber: Effect of printing orientation on tensile performance. *Polym. Adv. Technol.* **2019**, *30*, 910–922. [[CrossRef](#)]
21. Ambone, T.; Torris, A.; Shanmuganathan, K. Enhancing the mechanical properties of 3D printed polylactic acid using nanocellulose. *Polym. Eng. Sci.* **2020**, *60*, 1842–1855. [[CrossRef](#)]
22. Wang, Q.; Ji, C.; Sun, L.; Sun, J.; Liu, J. Cellulose Nanofibrils Filled Poly(Lactic Acid) Biocomposite Filament for FDM 3D Printing. *Molecules* **2020**, *25*, 2319. [[CrossRef](#)]
23. Mazzanti, V.; Malagutti, L.; Mollica, F. FDM 3D Printing of Polymers Containing Natural Fillers: A Review of their Mechanical Properties. *Polymers* **2019**, *11*, 1094. [[CrossRef](#)]
24. Rech, F.; Silva, S.M.D.; Roldo, L.; Oliveira, J.M.; Silva, F.P. Formulação e caracterização de potenciais filamentos compósitos de PLA e talos de tabaco para aplicação em manufatura aditiva. *Rev. Mater.* **2020**, *26*, e12988.
25. Ngo, T.D.; Kashani, A.; Imbalzano, G.; Nguyen, K.T.; Hui, D. Additive manufacturing (3D printing): A review of materials, methods, applications and challenges. *Compos. B. Eng.* **2018**, *143*, 172–196.
26. Vyavahare, S.; Teraiya, S.; Panghal, D.; Kumar, S. Fused deposition modelling: A review. *Rapid Prototyp. J.* **2019**, *26*, 176–201. [[CrossRef](#)]
27. Bardot, M.; Schulz, M.D. Biodegradable Poly(Lactic Acid) Nanocomposites for Fused Deposition Modeling 3D Printing. *Nanomaterials* **2020**, *10*, 2567. [[CrossRef](#)]
28. Das, A.K.; Agar, D.A.; Rudolfsson, M.; Larsson, S.H. A review on wood powders in 3D printing: Processes, properties and potential applications. *J. Mater. Res. Technol.* **2021**, *15*, 241–255.
29. Stoof, D.; Pickering, K.; Zhang, Y. Fused Deposition Modelling of Natural Fibre/Poly(lactic acid) Composites. *J. Compos. Sci.* **2017**, *1*, 8. [[CrossRef](#)]
30. Xie, G.; Zhang, Y.; Lin, W. Plasticizer Combinations and Performance of Wood Flour–Poly(Lactic Acid) 3D Printing Filaments. *BioResources* **2017**, *12*, 6736–6748. [[CrossRef](#)]
31. Guo, R.; Ren, Z.; Bi, H.; Song, Y.; Xu, M. Effect of toughening agents on the properties of poplar wood flour/poly (lactic acid) composites fabricated with Fused Deposition Modeling. *Eur. Polym. J.* **2018**, *107*, 34–45. [[CrossRef](#)]
32. Martikka, O.; Kärki, T.; Wu, Q.L. Mechanical Properties of 3D-Printed Wood-Plastic Composites. *Key Eng. Mater.* **2018**, *777*, 499–507. [[CrossRef](#)]
33. Yang, T.-C. Effect of Extrusion Temperature on the Physico-Mechanical Properties of Unidirectional Wood Fiber-Reinforced Poly(lactic acid) Composite (WFRPC) Components Using Fused Deposition Modeling. *Polymers* **2018**, *10*, 976. [[CrossRef](#)]
34. Ayrlmis, N.; Kariz, M.; Kwon, J.H.; Kuzman, M.K. Effect of printing layer thickness on water absorption and mechanical properties of 3D-printed wood/PLA composite materials. *Int. J. Adv. Manuf. Technol.* **2019**, *102*, 2195–2200. [[CrossRef](#)]
35. Guessasma, S.; Belhabib, S.; Nouri, H. Microstructure and Mechanical Performance of 3D Printed Wood-PLA/PHA Using Fused Deposition Modelling: Effect of Printing Temperature. *Polymers* **2019**, *11*, 1778. [[CrossRef](#)]
36. Le Guen, M.-J.; Hill, S.; Smith, D.; Theobald, B.; Gaugler, E.; Barakat, A.; Mayer-Laigle, C. Influence of Rice Husk and Wood Biomass Properties on the Manufacture of Filaments for Fused Deposition Modeling. *Front. Chem.* **2019**, *7*, 735. [[CrossRef](#)]
37. Bhagia, S.; Lowden, R.R.; Erdman, D., III; Rodriguez, M., Jr.; Haga, B.A.; Solano, I.R.M.; Gallego, N.C.; Pu, Y.; Muchero, W.; Kunc, V.; et al. Tensile properties of 3D-printed wood-filled PLA materials using poplar trees. *Appl. Mater. Today* **2020**, *21*, 100832. [[CrossRef](#)]
38. Estakhrianhaghghi, E.; Mirabolghasemi, A.; Zhang, Y.; Lessard, L.; Akbarzadeh, A. 3D-Printed Wood-Fiber Reinforced Architected Cellular Composites. *Adv. Eng. Mater.* **2020**, *22*, 2000565.
39. Kumar, S.D.; Venkadeshwaran, K.; Aravindan, M. Fused deposition modelling of PLA reinforced with cellulose nano-crystals. *Mater. Today Proc.* **2020**, *33*, 868–875. [[CrossRef](#)]
40. Ma, S.; Kou, L.; Zhang, X.; Tan, T. Energy grass/poly(lactic acid) composites and pretreatments for additive manufacturing. *Cellulose* **2020**, *27*, 2669–2683. [[CrossRef](#)]
41. Da Silva, S.M.; Antunes, T.; Costa, M.; Oliveira, J. Cork-like filaments for Additive Manufacturing. *Addit. Manuf.* **2020**, *34*, 101229. [[CrossRef](#)]
42. Yang, F.; Zeng, J.; Long, H.; Xiao, J.; Luo, Y.; Gu, J.; Zhou, W.; Wei, Y.; Dong, X. Micrometer Copper-Zinc Alloy Particles-Reinforced Wood Plastic Composites with High Gloss and Antibacterial Properties for 3D Printing. *Polymers* **2020**, *12*, 621. [[CrossRef](#)]
43. Yang, T.-C.; Yeh, C.-H. Morphology and Mechanical Properties of 3D Printed Wood Fiber/Poly(lactic acid) Composite Parts Using Fused Deposition Modeling (FDM): The Effects of Printing Speed. *Polymers* **2020**, *12*, 1334. [[CrossRef](#)]
44. Figueroa-Velarde, V.; Diaz-Vidal, T.; Cisneros-López, E.O.; Robledo-Ortiz, J.R.; López-Naranjo, E.J.; Ortega-Gudiño, P.; Rosales-Rivera, L.C. Mechanical and Physicochemical Properties of 3D-Printed Agave Fibers/Poly(lactic acid) Biocomposites. *Materials* **2021**, *14*, 3111.

45. Jing, H.; He, H.; Liu, H.; Huang, B.; Zhang, C. Study on properties of polylactic acid/lemongrass fiber biocomposites prepared by fused deposition modeling. *Polym. Compos.* **2020**, *42*, 973–986. [[CrossRef](#)]
46. Sekar, V.; Zarrouq, M.; Namasivayam, S.N. Development and Characterization of Oil Palm Empty Fruit Bunch Fibre Reinforced Polylactic Acid Filaments for Fused Deposition Modeling. *J. Mech. Eng.* **2021**, *18*, 89–107.
47. Yu, W.; Dong, L.; Lei, W.; Zhou, Y.; Pu, Y.; Zhang, X. Effects of Rice Straw Powder (RSP) Size and Pretreatment on Properties of FDM 3D-Printed RSP/Poly(lactic acid) Biocomposites. *Molecules* **2021**, *26*, 3234. [[CrossRef](#)]
48. Fico, D.; Rizzo, D.; De Carolis, V.; Montagna, F.; Palumbo, E.; Corcione, C.E. Development and characterization of sustainable PLA/Olive wood waste composites for rehabilitation applications using Fused Filament Fabrication (FFF). *J. Build. Eng.* **2022**, *56*, 104673. [[CrossRef](#)]
49. Inseemesak, B.; Siripaiboon, C.; Somkeattikul, K.; Attasophonwattana, P.; Kiatiwat, T.; Punsuvon, V.; Areeprasert, C. Biocomposite fabrication from pilot-scale steam-exploded coconut fiber and PLA/PBS with mechanical and thermal characterizations. *J. Clean. Prod.* **2022**, *379*, 134517.
50. Lohar, D.; Nikalje, A.; Damle, P. Development and testing of hybrid green polymer composite (HGPC) filaments of PLA reinforced with waste bio fillers. *Mater. Today Proc.* **2022**, *62*, 818–824.
51. Lohar, D.; Nikalje, A.; Damle, P. Synthesis and characterization of PLA hybrid composites using bio waste fillers. *Mater. Today Proc.* **2023**, *72*, 2155–2162.
52. Mansingh, B.B.; Binoj, J.S.; Tan, Z.Q.; Eugene, W.W.L.; Amornsakchai, T.; Hassan, S.A.; Goh, K.L. Comprehensive characterization of raw and treated pineapple leaf fiber/polylactic acid green composites manufactured by 3D printing technique. *Polym. Compos.* **2022**, *43*, 6051–6061.
53. Müller, M.; Šleger, V.; Kolář, V.; Hromasová, M.; Piš, D.; Mishra, R.K. Low-Cycle Fatigue Behavior of 3D-Printed PLA Reinforced with Natural Filler. *Polymers* **2022**, *14*, 1301. [[CrossRef](#)]
54. Palaniyappan, S.; Veeman, D.; Sivakumar, N.K.; Natrayan, L. Development and optimization of lattice structure on the walnut shell reinforced PLA composite for the tensile strength and dimensional error properties. *Structures* **2022**, *45*, 163–178. [[CrossRef](#)]
55. Scaffaro, R.; Gulino, E.F.; Citarrella, M.C.; Maio, A. Green Composites Based on *Hedysarum coronarium* with Outstanding FDM Printability and Mechanical Performance. *Polymers* **2022**, *14*, 1198. [[CrossRef](#)]
56. Shahar, F.S.; Sultan, M.T.H.; Safri, S.N.A.; Jawaid, M.; Talib, A.R.A.; Basri, A.A.; Shah, A.U.M. Fatigue and impact properties of 3D printed PLA reinforced with kenaf particles. *J. Mater. Res. Technol.* **2022**, *16*, 461–470.
57. Sun, Y.; Wang, Y.; Mu, W.; Zheng, Z.; Yang, B.; Wang, J.; Zhang, R.; Zhou, K.; Chen, L.; Ying, J.; et al. Mechanical properties of 3D printed micro-nano rice husk/polylactic acid filaments. *J. Appl. Polym. Sci.* **2022**, *139*, e52619. [[CrossRef](#)]
58. Basnett, P.; Ravi, S.; Roy, I. 8—Natural bacterial biodegradable medical polymers: Polyhydroxyalkanoates. In *Science and Principles of Biodegradable and Bioresorbable Medical Polymers*; Zhang, X., Ed.; Woodhead Publishing: Sawston, UK, 2017; pp. 257–277.
59. *ASTM D638-14*; Standard Test Method for Tensile Properties of Plastics. ASTM International: West Conshohocken, PA, USA, 2015.
60. *ISO 527-1:2019*; Plastics—Determination of Tensile Properties. International Organization for Standardization: Geneva, Switzerland, 2019.
61. *GB/T 1040-92*; Plastics-Determination of Tensile Properties. Standardization Administration of China: Beijing, China, 1992.
62. *GB/T 24508-2009*; Wood-Plastic Composite Flooring. Standardization Administration of China: Beijing, China, 2009.
63. *ASTM D790-17*; Standard Test Methods for Flexural Properties of Unreinforced and Reinforced Plastics and Electrical Insulating Materials. ASTM International: West Conshohocken, PA, USA, 2017.
64. *ISO 178*; Plastics—Determination of Flexural Properties. International Organization for Standardization: Geneva, Switzerland, 2019.

Disclaimer/Publisher’s Note: The statements, opinions and data contained in all publications are solely those of the individual author(s) and contributor(s) and not of MDPI and/or the editor(s). MDPI and/or the editor(s) disclaim responsibility for any injury to people or property resulting from any ideas, methods, instructions or products referred to in the content.